Technical University of Denmark

DTU

Local Chemical Reactivity of a Metal Alloy Surface

Hammer, Bjørk; Scheffler, Matthias

Link back to DTU Orbit

DTU Library
Technical Information Center of Denmark

Local Chemical Reactivity of a Metal Alloy Surface

B. Hammer[1,2] and M. Scheffler[1]

[1]*Fritz-Haber-Institut der Max-Planck-Gesellschaft, Faradayweg 4-6, D-14195 Berlin-Dahlem, Germany*
[2]*Center for Atomic-Scale Materials Physics (CAMP) and Physics Department, Technical University of Denmark,*
DK-2800 Lyngby, Denmark

The chemical reactivity of a metal alloy surface is studied by density functional theory investigating the interaction of H_2 with NiAl(110). The energy barrier for H_2 dissociation is largely different over the Al and Ni sites without, however, reflecting the barriers over the single component metal surfaces. This local chemical behavior is due to the covalent nature of the (H_2 σ_g)-(Ni $3d_{z^2}$) and (H_2 σ_u^*)-(Ni $3d_{xz}$) interactions. Thus, it cannot be described in terms of the Harris-Andersson model (i.e., Pauli repulsion and its weakening by empty d states).

Understanding and controlling the physical and chemical mechanisms behind reactions in heterogeneous catalysis stands as one of the long term goals of surface science. Much progress has been made in developing simple, intuitive pictures of how adsorbates interact with solid surfaces [1,2]. However, theoretical investigations of the chemical reactivity of alloy and bimetal surfaces is very scarce, despite the fact that many real catalysts consist of solid surfaces of several metallic components [3]. The present Letter starts bridging this gap, by presenting the first density functional theory (DFT) investigation of molecular dissociation on an ordered alloy, namely, H_2 on NiAl(110).

It has been shown previously [4] that the bulk properties of NiAl are well described in terms of a *collective* electron band structure with completely filled Ni d bands. As shown below, the situation is noticeably different at the surface, where the electronic properties at the Ni and Al sites turn out to be distinguishable. Performing a DFT study of the dissociative adsorption of an H_2 molecule on the ordered alloy NiAl(110) we demonstrate that and explain why the different substrate atoms behave chemically very differently at the surface. The energy barrier against dissociative adsorption is 1.3 eV when the molecule impinges over the Al site and only 0.5 eV over the Ni site. Although this difference is significant, the energy barrier over the Ni site remains considerable. This implies that the chemical reactivity is still characteristic of the alloy and not of a clean Ni surface, for which we find no energy barrier. Furthermore, we show that the difference in the energy barriers for H_2 dissociation over Al and Ni sites can be understood in terms of a covalent interaction of the H_2 molecular bonding and antibonding states with the local density of states at the two sites. In particular, we find that the (H_2 σ_g)-(Ni $3d_{z^2}$) and ($H_2\sigma_u^*$)-(Ni $3d_{xz}$) interactions (z being the surface normal and with the H_2 axis parallel to the surface and along x) are strong and have their antibonding combinations partially depopulated. As a consequence, the H_2-surface interaction reflects a stronger bonding contribution over the Ni sites than over the Al sites. These results are then compared to

those for the single component Ni(111) and Cu(111) surfaces which also show a significant covalent interaction between the molecule and the surface at close proximity, where the energy barrier occurs. The covalent interaction found in the present Letter has been anticipated by Nørskov and co-workers [5,6] in the construction of H_2-metal model potentials. On the other hand, the often celebrated Harris-Andersson concept [7] that empty d states reduce the Pauli repulsion between the molecule and the surface, which certainly applies at larger distances, turns out to be of no relevance in the discussion of whether barriers exist or not as these build up at close distances where the covalent effects dominate.

For the present investigations we choose DFT calculations with the exchange-correlation energy functional of the generalized gradient approximation (GGA) [8] applied non-self-consistently [9] to the charge density found in the local density approximation (LDA) [10]. Similar calculations have proven successful in describing the H_2 dissociation on Cu(111), leading to almost quantitative agreement between calculated and measured barrier heights [11,12].

The ordered alloy NiAl crystallizes in the CsCl structure. Its (110) surface thus contains the same number of Ni and Al atoms. In our calculations we describe the NiAl(110) substrate by a slab of five NiAl layers using the theoretical lattice constant 2.845 Å. The geometry of the clean NiAl(110) surface exhibits a rippled relaxation which is calculated to be -7.0% and $+4.5\%$ of the unrelaxed interlayer separation (2.0 Å) for the surface Ni and Al atoms, respectively [13,14]. For the study of the H_2-substrate interaction we use a $c(2 \times 2)$ surface cell with two Ni and two Al atoms leading to a H_2-H_2 separation of 4.9 Å, which implies a rather weak interaction between different supercells. The Brillouin zone sampling is performed with 16 special **k** points (4 **k** points in the irreducible wedge). The choice of pseudopotentials, plane wave basis, kT_e, and minimization algorithm is the same as in Ref. [14], where the method proved successful in describing properties of bulk NiAl and its (110) surface. The rippled substrate surface is kept frozen during the interaction with the H_2

molecule, because a geometry change would happen on a slower time scale than the dissociation event. We note, however, that as the relaxations of the clean and H covered NiAl(110) are noticeably different [14], the H_2/NiAl(110) system might show similar phenomena in associative desorption as found for H_2 at Si(100) [15,16].

Figure 1(a) presents the potential energy curves of the dissociation of an H_2 molecule held parallel to the surface and being centered over the Al and Ni sites, respectively [Figs. 1(b) and 1(c)]. The in-plane orientation of the H_2 molecule is chosen so that both pathways lead directly into the equilibrium (1×1) structure of dissociated atomic hydrogen in the Ni-Ni bridge [Fig. 1(d)] reported in Ref. [14]. By considering two pathways with the same as-dissociated hydrogen positions, we obtain potential energy curves that reflect the *differences* in molecule-surface interaction most clearly. Inspection of the intramolecular forces suggests that over the Al sites, the transition state is at $1.57 < Z < 1.75$ Å, while over the Ni sites it is at $1.19 < Z < 1.39$ Å. The energy barrier for H_2 dissociation over the Al site is therefore about 1.3 eV over the Al site while about 0.5 eV over the Ni site. This demonstrates that the molecule-surface interaction depends most sensitively on the point of impact. Judging from the sizable activation barrier over the Ni sites we note that the interaction does not reflect the behavior of a pure Ni surface, for which a vanishing barrier would be expected from experimental observations [17] and for which no barrier is found in the DFT-GGA calculation for Ni(111) reported below.

In order to elucidate the mechanism behind the different interactions at the two sites, we consider the density of
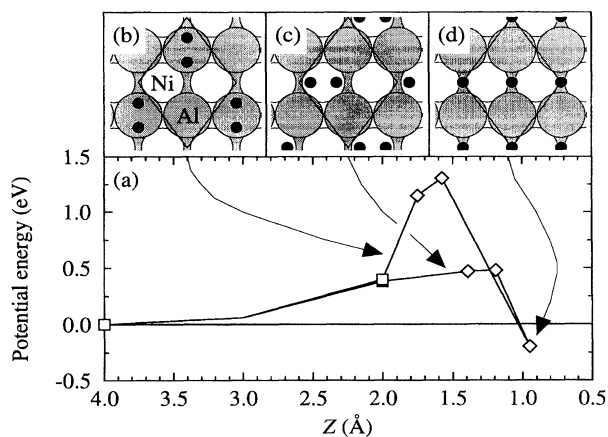
states (DOS) at the energy ε (relative to the Fermi level) projected on the localized orbital ϕ_a:

$$n_a(\varepsilon) = \sum_i \int |\langle \phi_a | \psi_i(\mathbf{k}) \rangle|^2 \delta[\varepsilon - \varepsilon_i(\mathbf{k})] \, d\mathbf{k}, \quad (1)$$

where i is the band index running over all bands, $\mathbf{k}$ is integrated over the entire Brillouin zone (BZ), $\psi_i(\mathbf{k})$ are the Kohn-Sham wave functions, and $\varepsilon_i(\mathbf{k})$ are the corresponding single particle energies. Because of the finite $\mathbf{k}$-point sampling in our calculation, the BZ integral is replaced with a discrete sum, and the δ function is for convenience replaced with a Gaussian of width 0.25 eV.

For ϕ_a we choose the H_2 molecular bonding (σ_g) and antibonding (σ_u^*) orbitals that are constructed as normalized linear combinations of the hydrogen s orbitals [18], ϕ_s^H, centered at the positions of the two hydrogen atoms $\mathbf{R}_1$ and $\mathbf{R}_2$:

$$\phi_{\sigma_g}(\mathbf{r}) = c_1 \{ \phi_s^H(\mathbf{r} - \mathbf{R}_1) + \phi_s^H(\mathbf{r} - \mathbf{R}_2) \},$$

$$\phi_{\sigma_u^*}(\mathbf{r}) = c_2 \{ \phi_s^H(\mathbf{r} - \mathbf{R}_1) - \phi_s^H(\mathbf{r} - \mathbf{R}_2) \}, \quad (2)$$

where c_1 and c_2 are chosen to ensure normalization.

In Figs. 2 and 3 the projected DOS, $n_{\sigma_g}(\varepsilon)$ and $n_{\sigma_u^*}(\varepsilon)$, are shown for five different positions along the two pathways of Fig. 1. For both pathways, the H_2 bonding level is seen to initially broaden and shift down in energy when the molecule approaches the surface. This behavior is readily understood within a Newns-Anderson model [19] as originating from weak coupling of an adsorbate level in resonance with a *broad* continuum of states, and has been demonstrated in jellium calculations by Lundqvist and co-workers [5,20]. When the molecular bond is succeedingly weakened, the H_2 bonding level shifts up and finally meets the antibonding level. In addition to this main feature, also a smaller resonance is observed. This appears in Figs. 2(b) and 3(b) just below the Fermi energy and moves up through the Fermi level as the dissociation is completed. This resonance has antibonding character between the molecule and the surface, as will be apparent below.
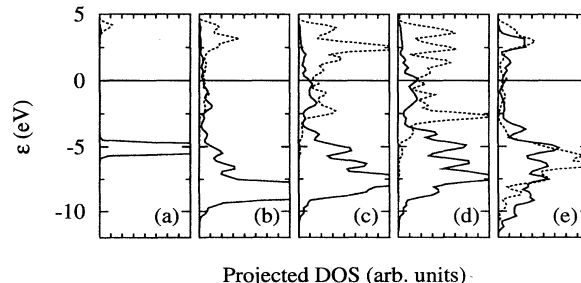

FIG. 1. (a) The potential energy of H_2 dissociating over NiAl(110) versus the height Z of the H_2 center of mass from the plane of the unrelaxed surface atomic position. The upper (lower) curve is a guide to the eye connecting points for H_2 over the Al (Ni) site. The geometries have been optimized with respect to the H-H separation b at fixed Z ($\square$) or with respect to Z at fixed b ($\diamond$). (b) H_2 ($\bullet$ pairs) over the Al sites (shaded circles) of the NiAl(110). The $c(2 \times 2)$ unit cell is indicated. (c) H_2 over the Ni sites (open circles). (d) (1×1)-H/NiAl(110).

Projected DOS (arb. units)

FIG. 2. H_2 dissociation over the Al: Molecular bonding $n_{\sigma_g}(\varepsilon)$ (solid curve) and antibonding, $n_{\sigma_u^*}(\varepsilon)$, (dashed curve) projected DOS at the five positions indicated in Fig. 1(a). Dissociation proceeds from left to right. The (b, Z) coordinates are (a) (0.78, 4.0 Å), (b) (0.81, 2.0 Å), (c) (1.2, 1.75 Å), (d) (1.5, 1.57 Å), and (e) (2.845, 0.95 Å).
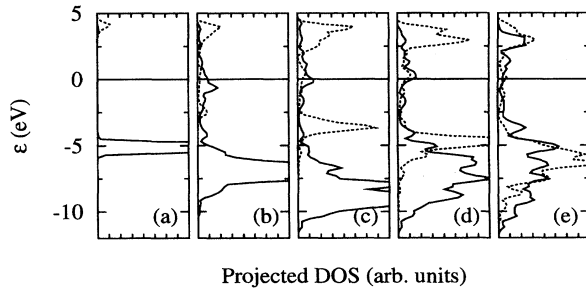
Projected DOS (arb. units)

FIG. 3. Same as Fig. 2 but for H_2 dissociation over the Ni. The (b, Z) coordinates are (a) (0.78, 4.0 Å), (b) (0.81, 2.0 Å), (c) (1.0, 1.39 Å), (d) (1.5, 1.19 Å), and (e) (2.845, 0.95 Å).

The interaction of the H_2 σ_u^* orbital with the metal states shows up in Figs. 2 and 3 noticeably different over the two different sites. For the H_2 over the Al site, mainly a broad $n_{\sigma_u^*}$ resonance (dashed curve in Fig. 2) evolves. This can be understood as due to the interaction with a broad continuum of substrate states. For H_2 over the Ni site, however, two well-separated narrow peaks evolve in $n_{\sigma_u^*}$ (dashed curve in Fig. 3). This is the signature of strong covalent coupling between an adsorbate level and a *narrow* continuum.

In order to achieve information about the chemical bonding character of the individual resonances in Figs. 2 and 3 we proceed by looking at the DOS projected onto three-center orbitals. We define

$$\xi(H_2 \; \sigma_u^*, Ni \; 3d_{xz})(\mathbf{r}) = c_3[\phi_{\sigma_u^*}(\mathbf{r}) + \chi \phi_{3d_{xz}}^{Ni}(\mathbf{r} - \mathbf{R}_{Ni})],$$

$$\xi^*(H_2 \; \sigma_u^*, Ni \; 3d_{xz})(\mathbf{r}) = c_4[\phi_{\sigma_u^*}(\mathbf{r}) - \chi \phi_{3d_{xz}}^{Ni}(\mathbf{r} - \mathbf{R}_{Ni})],$$

$$(3)$$

where $\phi_{3d_{xz}}^{Ni}$ is the atomic Ni $3d_{xz}$ orbital [18], $\mathbf{R}_{Ni}$ is the position of the surface Ni atom, $\chi = \mathrm{sgn}(\langle \phi_{\sigma_u^*} | \phi_{3d_{xz}}^{Ni} \rangle)$, and c_3 and c_4 are normalization constants. Orbitals being bonding (ξ) and antibonding (ξ^*) between the molecule and the surface, but involving other Ni or Al atomic orbitals, are defined analogously to Eq. (3).

Figures 4 and 5 display the DOS of Figs. 2(c) and 3(c), respectively, projected onto three-center orbitals as defined above. The chemical nature of the individual DOS peaks in Figs. 2 and 3 can now be addressed. The small resonance near the Fermi level in $n_{\sigma_g}(\varepsilon)$ is of $\xi^*(H_2 \; \sigma_g, Al \; 3s)$ character over the Al site and of $\xi^*(H_2 \; \sigma_g, Ni \; 3d_{z^2})$ character over the Ni site. It is seen that this molecule-surface antibonding resonance has a large share of its weight *above* the Fermi level when the dissociation takes place over the Ni site. This means that the molecule interacts in a stronger bonding manner with the surface when approaching over the Ni site than over the Al site. Consequently, the approach over the Ni site is energetically preferred.

The detailed behavior of $n_{\sigma_u^*}$ is also revealed by Figs. 4 and 5. Over the Al site the small peaks at -2 and 4 eV overlaying the main resonance at 2.5 eV are seen to orig-
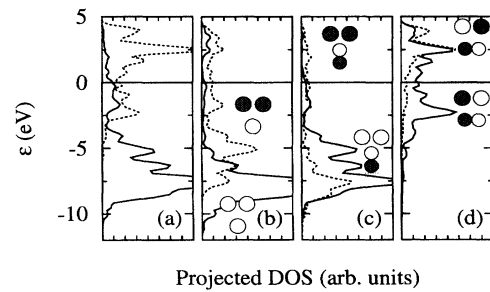

Projected DOS (arb. units)

FIG. 4. H_2 over the Al at $(b, Z) = (1.2, 4.0$ Å): The solid and dashed curves, respectively, show the DOS projected onto (a) ϕ_{σ_g} and $\phi_{\sigma_u^*}$, (b) $\xi(H_2 \; \sigma_g, Al \; 3s)$ and $\xi^*(H_2 \; \sigma_g, Al \; 3s)$, (c) $\xi(H_2 \; \sigma_g, Al \; 3p_z)$ and $\xi^*(H_2 \; \sigma_g, Al \; 3p_z)$, and (d) $\xi(H_2 \; \sigma_u^*, Al \; 3p_y)$ and $\xi^*(H_2 \; \sigma_u^*, Al \; 3p_y)$. In the symbolic sketches of the orbitals the two hydrogen s orbitals are depicted atop a substrate state. White (gray) represents positive (negative) sign.

inate from the splitting of the $\xi(H_2 \; \sigma_u^*, Al \; 3p_y)$ and the $\xi^*(H_2 \; \sigma_u^*, Al \; 3p_y)$ DOS. Over the Ni site it is the splitting of the $\xi(H_2 \; \sigma_u^*, Ni \; 3d_{xz})$ and the $\xi^*(H_2 \; \sigma_u^*, Ni \; 3d_{xz})$ DOS which completely dominates $n_{\sigma_u^*}$. Again, the degree to which the molecule-surface interaction (now through the intramolecular antibonding level) is bonding determines which reaction pathway is energetically preferred for dissociation. The stronger splitting over the Ni site therefore facilitates the dissociation. The present argumentation is independent of whether the Ni $3d$ states involved in the molecule-surface interaction are initially filled or empty. Thus, while asymptotically for large distances the interaction between a closed shell molecule and a metal surface may be affected by the Pauli repulsion between the filled molecular and substrate orbitals and the presence of a high and empty DOS at the Fermi level (as described by Harris and Andersson [7]) this effect is not important at distances close to the surface, where the dissociation energy barriers are typically found.

In order to complement the findings of the importance of the $(H_2 \; \sigma_g)$-$(Ni \; 3d_{z^2})$ and $(H_2 \; \sigma_u^*)$-$(Ni \; 3d_{xz})$ interactions on NiAl(110), we have performed DFT-GGA calculations for H_2 dissociation over Ni(111) and Cu(111).
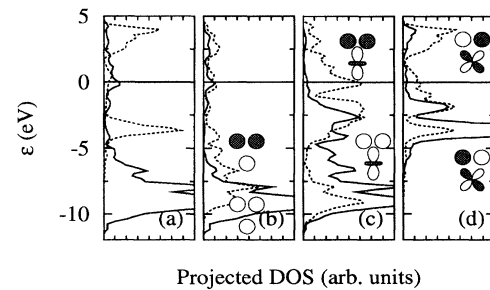

Projected DOS (arb. units)

FIG. 5. H_2 over the Ni at $(b, Z) = (1.0, 1.39$ Å): The solid and dashed curves, respectively, show the DOS projected onto (a) ϕ_{σ_g} and $\phi_{\sigma_u^*}$, (b) $\xi(H_2 \; \sigma_g, Ni \; 4s)$ and $\xi^*(H_2 \; \sigma_g, Ni \; 4s)$, (c) $\xi(H_2 \; \sigma_g, Ni \; 3d_{z^2})$ and $\xi^*(H_2 \; \sigma_g, Ni \; 3d_{z^2})$, and (d) $\xi(H_2 \; \sigma_u^*, Ni \; 3d_{xz})$ and $\xi^*(H_2 \; \sigma_u^*, Ni \; 3d_{xz})$.

For the geometry we choose H_2 parallel to the surfaces, centered over the Ni and Cu atoms, respectively, and adsorbing dissociatively directly into the threefold hollow sites of a $(\sqrt{3} \times \sqrt{3})$ surface cell on a 4-layer slab (54 **k** points in the BZ). While the energy barrier against dissociation is 0.5 eV on Cu(111) [11] it is absent on Ni(111).

Figures 6 and 7 show the H_2 σ_g and H_2 σ_u^* projected DOS over Ni(111) and Cu(111). Clearly, over both surfaces the σ_u^* projected DOS evolves into two well-separated narrow peaks. Also apparent is that a small peak in $n_{\sigma_g}(\varepsilon)$ evolves and goes through the Fermi level as the dissociation proceeds. The major difference between the dissociation on the Ni(111) and the Cu(111) can be summarized as follows. On Ni, the $\xi^*(H_2 \ \sigma_u^*, Ni \ 3d_{xz})$ DOS is almost empty all along the reaction and the $\xi^*(H_2 \ \sigma_g, Ni \ 3d_{z^2})$ DOS goes through the Fermi level at an early stage. On Cu, on the other hand, the $\xi^*(H_2 \ \sigma_u^*, Cu \ 3d_{xz})$ DOS has a considerable filling all along the reaction and the $\xi^*(H_2 \ \sigma_g, Cu \ 3d_{z^2})$ DOS remains largely filled. This difference arises due to the difference in the positions of the substrate d levels relative to the Fermi level on the two surfaces [Figs. 6(a) and 7(a)] and has as a consequence that Ni acts with much more molecule-surface bonding character than does Cu. Thus covalent effects involving the molecular states and the metal d states explain the calculated and observed differences in barrier heights. That the same behavior appears to be consistent with the Harris-Andersson picture is only because the energetically higher Ni $3d$ bands compared to the Cu $3d$ bands lead to d holes for Ni compared to none for Cu. However, as shown for H_2 over NiAl(110) even completely filled d bands cause an attractive molecule-surface interaction at close distances and therefore no picture invoking a particular role of the d holes applies to the H_2-metal systems.

In summary, we have presented the first density functional theory calculation of dissociative adsorption of H_2 on a metal alloy NiAl(110). The alloy is found to act chemically very locally, exhibiting largely varying barrier heights over Ni and Al sites. Both barriers being con-
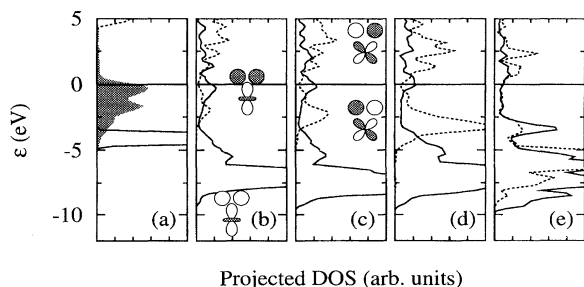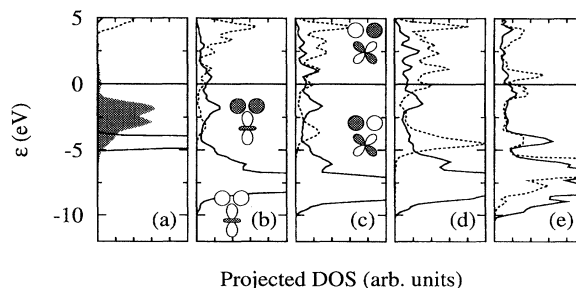

Projected DOS (arb. units)

FIG. 7.   Same as Fig. 6 but for H_2 dissociation over Cu(111).

siderable. The barrier difference is explained in terms of the covalent coupling between both the bonding and the antibonding molecular orbital and the Ni $3d$ states. This chemical picture also expounds the difference in H_2 dissociation barriers observed on pure Ni and Cu surfaces.

[1]   R. Hoffmann, Rev. Mod. Phys. **60**, 601 (1988).
[2]   J. K. Nørskov, Rep. Prog. Phys. **53**, 1253 (1990).
[3]   G. A. Somorjai, *Introduction to Surface Chemistry and Catalysis* (John Wiley & Sons, New York, 1994).
[4]   S. C. Lui *et al.,* Phys. Rev. B **42**, 1582 (1990).
[5]   B. I. Lundqvist, O. Gunnarsson, H. Hjelmberg, and J. K. Nørskov, Surf. Sci. **89**, 196 (1979).
[6]   J. K. Nørskov, J. Chem. Phys. **90**, 7461 (1989).
[7]   J. Harris and S. Andersson, Phys. Rev. Lett. **55**, 1583 (1985).
[8]   J. P. Perdew *et al.,* Phys. Rev. B **46**, 6671 (1992).
[9]   B. Hammer, K. W. Jacobsen, and J. K. Nørskov, Phys. Rev. Lett. **70**, 3971 (1993).
[10] D. M. Ceperley and B. J. Alder, Phys. Rev. Lett. **45**, 566 (1980); J. P. Perdew and A. Zunger, Phys. Rev. B **23**, 5048 (1981).
[11] B. Hammer, M. Scheffler, K. W. Jacobsen, and J. K. Nørskov, Phys. Rev. Lett. **73**, 1400 (1994).
[12] A. Gross, B. Hammer, M. Scheffler, and W. Brenig, Phys. Rev. Lett. **73**, 3121 (1994).
[13] M. H. Kang and E. J. Meele, Phys. Rev. B **36**, 7371 (1987).
[14] A. Hanbicki, A. P. Baddorf, E. W. Plummer, B. Hammer, and M. Scheffler, Surf. Sci. (to be published).
[15] P. Kratzer, B. Hammer, and J. K. Nørskov, Chem. Phys. Lett. **229**, 645 (1994).
[16] E. Pehlke and M. Scheffler, Phys. Rev. Lett. **74**, 952 (1995).
[17] H. J. Robota *et al.,* Surf. Sci. **155**, 101 (1985).
[18] All atomic wave functions are truncated at 2 bohrs in order to lower their overlap.
[19] D. M. Newns, Phys. Rev. **178**, 1123 (1969).J. K. Nørskov, A. Houmøller, P. Johansson, and B. I. Lundqvist, Phys. Rev. Lett. **46**, 257 (1981).
[20] J. K. Nørskov, A. Houmøller, P. Johansson, and B. I. Lundqvist, Phys. Rev. Lett. **46**, 257 (1981).

Projected DOS (arb. units)

FIG. 6. H_2 dissociation over Ni(111): Bonding, $n_{\sigma_g}(\varepsilon)$, (solid curve) and antibonding, $n_{\sigma_u^*}(\varepsilon)$, (dashed curve) projected DOS. The chosen (b,Z) coordinates are (a) (0.8, 6 Å), (b) (0.8, 2.0 Å), (c) (0.9, 1.75 Å), (d) (1.2, 1.5 Å), and (e) (2.5, 0.9 Å). The position of the d bands at the clean surface is indicated by the shaded area in (a).
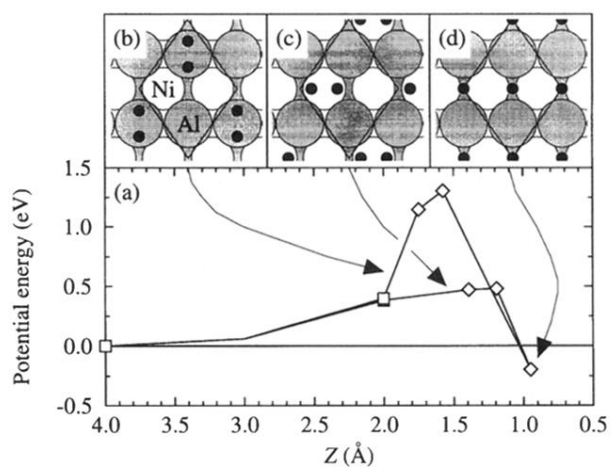
FIG. 1. (a) The potential energy of H_2 dissociating over NiAl(110) versus the height Z of the H_2 center of mass from the plane of the unrelaxed surface atomic position. The upper (lower) curve is a guide to the eye connecting points for H_2 over the Al (Ni) site. The geometries have been optimized with respect to the H-H separation b at fixed Z ($\square$) or with respect to Z at fixed b ($\diamond$). (b) H_2 ($\bullet$ pairs) over the Al sites (shaded circles) of the NiAl(110). The $c(2 \times 2)$ unit cell is indicated. (c) H_2 over the Ni sites (open circles). (d) (1×1)-H/NiAl(110).